THE JOURNAL OF BIOLOGICAL CHEMISTRY VOL. 288, NO. 23, pp. 16308–16320, June 7, 2013
Published in the U.S.A.

Heat Shock Protein 90 Functions to Stabilize and Activate the Testis-specific Serine/Threonine Kinases, a Family of Kinases Essential for Male Fertility*

Received for publication, April 16, 2013 Published, JBC Papers in Press, April 18, 2013, DOI 10.1074/jbc.M112.400978

Kula N. Jha[‡1], **Alyssa R. Coleman**[‡], **Lily Wong**[‡], **Ana M. Salicioni**[§], **Elizabeth Howcroft**[‡], **and Gibbes R. Johnson**[‡2]

From the [‡]*Division of Therapeutic Proteins, Center for Drug Evaluation and Research, Food and Drug Administration, Bethesda, Maryland 20892 and the* [§]*Department of Veterinary and Animal Sciences, University of Massachusetts, Amherst, Massachusetts 01003*

Background: Testis-specific serine/threonine kinases (TSSKs) are expressed in spermatids and are essential for male fertility.
Results: HSP90 inhibition results in increased ubiquitination and degradation of TSSKs and blocks catalytic activation of TSSK4 and -6.
Conclusion: The TSSK family of kinases is stabilized and activated by HSP90.
Significance: HSP90 may play a critical role in differentiation of spermatids and male fertility.

Spermiogenesis is characterized by a profound morphological differentiation of the haploid spermatid into spermatozoa. The testis-specific serine/threonine kinases (TSSKs) comprise a family of post-meiotic kinases expressed in spermatids, are critical to spermiogenesis, and are required for male fertility in mammals. To explore the role of heat shock protein 90 (HSP90) in regulation of TSSKs, the stability and catalytic activity of epitope-tagged murine TSSKs were assessed in 293T and COS-7 cells. TSSK1, -2, -4, and -6 (small serine/threonine kinase) were all found to associate with HSP90, and pharmacological inhibition of HSP90 function using the highly specific drugs 17-AAG, SNX-5422, or NVP-AUY922 reduced TSSK protein levels in cells. The attenuation of HSP90 function abolished the catalytic activities of TSSK4 and -6 but did not significantly alter the specific activities of TSSK1 and -2. Inhibition of HSP90 resulted in increased TSSK ubiquitination and proteasomal degradation, indicating that HSP90 acts to control ubiquitin-mediated catabolism of the TSSKs. To study HSP90 and TSSKs in germ cells, a mouse primary spermatid culture model was developed and characterized. Using specific antibodies against murine TSSK2 and -6, it was demonstrated that HSP90 inhibition resulted in a marked decrease of the endogenous kinases in spermatids. Together, our findings demonstrate that HSP90 plays a broad and critical role in stabilization and activation of the TSSK family of protein kinases.

During spermatogenesis, germ cells (spermatogonia) undergo several rounds of mitotic division to produce spermatocytes, which subsequently undergo two consecutive meiotic divisions to give rise to haploid round spermatids. Spermiogenesis is a poorly understood developmental cascade of events by which the round spermatids elongate, condense their nuclei, acquire flagellum and acrosome, and shed excess cytoplasm to form spermatozoa (1, 2). The cell differentiation during spermiogenesis also involves biochemical changes including, but not limited to, the protein composition (3) and decreases in transcription (4). The identification and functional characterization of the proteins that are exclusively expressed in spermatids will provide insights into understanding the molecular mechanisms underlying the process of spermiogenesis.

A number of protein kinases are expressed in male germ cells, and several of them are required for male fertility (5). For example, null male mice for CAMK4, casein kinase 2α' catalytic subunit, and cyclin-dependent kinase 2 (CDK2)[3] are infertile (6–8). The testis-specific serine/threonine kinases (TSSKs) are exclusively expressed in spermatids (9), and three of them, namely TSSK1, -2, and -6 (also known as small serine/threonine kinase (SSTK)), have been evaluated by genetic deletion in mice and shown to be essential for male fertility (10–12). The TSSK family consists of six members but TSSK5 does not appear to possess all the subdomains that are required for a kinase (9). The TSSKs have high homology to one another, with TSSK3 and -6 as the smallest members consisting of only N- and C-lobes of the kinase catalytic domain (9, 11). TSSK4 has a 13-amino acid extension at the N terminus, a 36-amino acid extension at the C terminus, and an insertion of 11 amino acids between the kinase subdomains VII and VIII in the C-lobe. TSSK1 and -2 are the largest members in the family, with C-ter-

* This work was supported in part by an appointment of A. R. C. to the ORISE Research Participation Program at the Center for Drug Evaluation and Research (CDER) administered by the Oak Ridge Institute for Science and Education through an agreement between the United States Department of Energy and CDER.

[1] To whom correspondence may be addressed: 29 Lincoln Dr., Bldg. 29A, HFD-122, Division of Therapeutic Proteins, Center for Drug Evaluation and Research, Food and Drug Administration, Bethesda, MD 20892. Tel.: 301-827-1761; Fax: 301-480-3256; E-mail: kula.jha@fda.hhs.gov.

[2] To whom correspondence should be addressed: 29 Lincoln Dr., Bldg. 29A, HFD-122, Division of Therapeutic Proteins, Center for Drug Evaluation and Research, Food and Drug Administration, Bethesda, MD 20892. Tel.: 301-827-1770; Fax: 301-480-3256; E-mail: gibbes.johnson@fda.hhs.gov.

[3] The abbreviations used are: CDK2, cyclin-dependent kinase 2; TSSK, testis-specific serine/threonine kinase; 17-AAG, 17-allylamino-17-demethoxygeldanamycin; HSP90, heat shock protein 90; SIP, small serine/threonine kinase (SSTK)-interacting protein; TSACC, TSSK6-activating co-chaperone; H1t, testis-specific histone H1; WB, Western blot; IP, immunoprecipitation.

minal kinase domain extensions of 94 and 87 amino acids, respectively. The targeted disruption of TSSK1/TSSK2 (double knock-out) in mice resulted in abnormal spermatid development, and the observed phenotype was associated with structural defects in mitochondrial sheath formation and the premature loss of the chromatoid body-derived ring structure in spermatids (10). Similarly, the development of spermatids was also impaired in TSSK6 knock-out animals and resulted in the production of morphologically abnormal sperm (11). Furthermore, TSSK6 null sperm were incapable of fusing with zona pellucida-free eggs (13).

The heat shock protein 90 (HSP90) chaperone machinery is a multipartner complex of proteins that often also contains HSP70, HOP, HSP40, P23, and/or CDC37 (14–17). Unlike the other major classes of HSPs, HSP90 preferentially interacts with a specific subset of proteins and is involved with maturation of signaling molecules including protein kinases, transcription factors, and hormone receptors (14, 15). HSP90 possesses an intrinsic ATPase activity that is required for mediating the necessary conformational changes in client proteins for activation (15, 17, 18) and is also important for stabilization of the HSP90 client proteins (19, 20). HSP90 inhibitors 17-allylamino-17-demethoxygeldanamycin (17-AAG) as well as other structurally distinct agents, including SNX-5422 (also known as PF-04929113) and NVP-AUY922, bind to the nucleotide binding pocket of HSP90 and inhibit the progression of the HSP90 complex toward the stabilizing form resulting in the degradation of the client proteins (16, 19, 21–23). It is well established that pharmacological inhibition of HSP90 can lead to degradation of a large variety of client proteins including kinases such as RAF kinase, ERBB2, AKT, v-SRC, and death domain kinase, the transcription factors mutants p53 and HIF-1α, the mineralocorticoid, glucocorticoid, and mutant androgen receptors, and others such as the cystic fibrosis transmembrane conductance regulator CFTR and huntingtin (19, 21, 24–32).

Recently we identified an HSP70 binding co-chaperone named small serine/threonine kinase (SSTK)-interacting protein (SIP; TSSK6-activating co-chaperone (TSACC)) that facilitates the HSP90-mediated activation of TSSK6 (33). However, it remained to be determined whether the role of HSP90 in activation was limited to TSSK6 or if the other TSSKs were also regulated by HSP90. Interestingly, male germ cells express the HSP90α (gene Hsp90aa1) isoform and targeted disruption of HSP90α in mice resulted in male infertility without any other obvious somatic defects (34). The spermatogenic cells failed to develop beyond meiosis in the HSP90α null mice, demonstrating that HSP90 is critical for meiosis in the male germ cells. To investigate whether HSP90 plays a broad role in the regulation of the TSSK family of post-meiotic kinases, we have performed a systematic analysis of the stability and activity of TSSK1, -2, -3, -4, and -6 using a panel of expression constructs containing the murine kinase cDNAs with a Myc epitope tag at the C terminus. When ectopically expressed in either 293T or COS-7 cells, TSSKs were found to be specifically stabilized by HSP90, and the catalytic activities of TSSK4 and -6 were demonstrated to require HSP90 function. Furthermore, TSSKs were subjected to ubiquitination, and HSP90 inhibition resulted in enhanced ubiquitination and subsequent proteasomal degradation. We developed a mouse spermatid primary culture model and confirmed that TSSK2 and -6 protein levels were reduced in mouse spermatids in response to HSP90 inhibition. Taken together, our data demonstrate that HSP90 regulates TSSKs by influencing their stability and/or activation and strongly suggests that HSP90 function is important for post-meiotic differentiation of spermatids and fertility in mammals.

EXPERIMENTAL PROCEDURES

Reagents—[^{32}P]ATP and enhanced chemiluminescence kit were purchased from PerkinElmer Life Sciences. Histone H2A and H1 were obtained from Upstate Biotechnology (Lake Placid, NY). The monoclonal antibody for TSSK2 (clone 1E12) was obtained from Novus Biologicals (Littleton, CO) and a rabbit polyclonal antibody for testis-specific histone H1 (H1t) was obtained from Abcam (Cambridge, MA). Myc (clone 9E-10) and HSP90 antibodies were purchased from Santa Cruz Biotechnology (Santa Cruz, CA). The monoclonal antibody (clone E7) against β-tubulin was obtained from the Developmental Studies Hybridoma Bank maintained by Department of Biological Sciences, University of Iowa. 17-AAG was purchased from Sigma, and the other two HSP90 inhibitors (SNX-5422 and NVP-AUY922) were purchased from Selleck (Houston, TX). Proteasomal inhibitors MG132 and epoxomicin were purchased from EMD Millipore (Billerica, MA). TRIzol reagent for RNA extraction was purchased from Invitrogen, and the Advantage RT-for-PCR kit for cDNA synthesis was purchased from Clontech (Mountain View, CA). All reagents were of analytical grade.

Kinase Expression Constructs—TSSKs and CDK2 cDNAs were inserted into pcDNA 3.1 myc/his (Invitrogen) using standard molecular biology techniques. The entire coding region for each construct was confirmed by DNA sequencing. HA-tagged wild type ubiquitin construct (pRK5-HA-ubiquitin WT) was obtained from Addgene (Cambridge, MA) (35).

Protein Expression in 293T and COS-7 Cells—Myc epitope-tagged TSSKs and CDK2 cDNA construct was transfected in 293T cells as described earlier (33). Transfections of Myc epitope-tagged TSSKs, CDK2, and HA-tagged ubiquitin in COS-7 cells were carried out using the DEAE-dextran chloroquine technique (36). When required, the cells were treated with 1 μM HSP90 inhibitor (17-AAG, SNX-5422, or NVP-AUY922) or DMSO (vehicle control). In some experiments, cells were also treated with proteasomal inhibitors (5 μM MG132 or 0.2 μM epoxomicin).

Western Blotting and Immunoprecipitation—Western blotting and immunoprecipitation (IP) were performed as described previously (33). Myc IP from denatured lysate for the ubiquitination assay, as depicted in Fig. 7, was performed following the protocol described by van de Kooij *et al.* (37). Briefly, COS-7 cells were lysed in 50 mM Tris-HCl, pH 8.0, 1% SDS, 10 mM DTT, and 0.5 mM EDTA and boiled for 10 min. The lysate was diluted by adding 9 volumes of Nonidet P-40 buffer (50 mM Tris-HCl, pH 7.4, 1% Nonidet P-40, 150 mM NaCl, 1 μg/ml aprotinin, 1 μg/ml leupeptin, 1 mM PMSF, 10 mM β-glycerophosphate, and 1 mM sodium orthovanadate) and cleared by centrifugation at 13,000 $\times$ *g* for 15 min. Myc IP from the cleared lysate was performed and analyzed by Western blotting.

Protein Kinase Assay—Kinase reactions were performed as described previously (33). Briefly, the reaction was carried out at room temperature for 30 min in buffer that contained 25 mM HEPES, pH 7.4, 10 mM $MgCl_2$, 10 mM $MnCl_2$, 2 mM EGTA, 30 μM ATP, 10 μCi of [γ-^{32}P]ATP, and a protein substrate. Histone H2A and histone H1 were used as the protein substrate for TSSKs and CDK2, respectively. Kinase reactions were terminated with Laemmli sample buffer, resolved in SDS-PAGE gels, and developed by autoradiography. In some experiments lysates were diluted before immunoprecipitation to achieve constant amounts of the Myc-tagged TSSKs in the immune complexes.

Quantitative RT-PCR—Cells were harvested, and RNA was extracted using TRIzol reagent according to the instructions from the manufacturer. RNA was reverse-transcribed to cDNA using Advantage RT-for-PCR kit (Clontech), and quantitative real-time PCR assays were performed in Bio-Rad iCycler using Bio-Rad kits with detection by SYBR Green dye following the instructions from the manufacturer. The sequences of RT-PCR primers were the following: TSSK1 (forward, 5′-AAA CTT GGG AGA GGG CTC AT-3′, and reverse, 5′-TGG CCA GAA TCT CAA TCT CC-3′); TSSK2 (forward, 5′-CCA CGC TCC AAG AAC CTA AC-3′, and reverse, 5′-GAA GGA GGC AGA AGA CAT GG-3′); TSSK3 (forward, 5′-GAT GCT GGA GTC AGC AGA TG-3′, and reverse, 5′-GGC AAT AGC GAA TAG CCT CA-3′); TSSK4 (forward, 5′-CTG TCA AGA TCA TCT CGA AG-3′, and reverse, 5′-GAG CCA CGT CCA AAA TGA TGT-3′); TSSK6 (forward, 5′-CGC TCA AGA TCA CGG ATT TC-3′, and reverse, 5′-AGG CTC CAC ACG TCG TAT TT-3′), and actin (forward, 5′-GAC GAT GCT CCC CGG GCT GTA TTC-3′, and reverse, 5′-TCT CTT GCT CTG GGC CTC GTC ACC-3′). The conditions used for the amplification were the following: 95 °C for 3 min; 95 °C for 10 s, 55 °C for 30 s, and 72 °C for 30 s for 40 cycles; 95 °C for 1 min; 55 °C for 1 min. Each assay was run in triplicate, and corresponding triplicates for amplifying the housekeeping gene (actin) were included in parallel. The CT values of a TSSK gene were normalized with actin and the $2^{-\Delta\Delta CT}$ method was used to calculate the relative expressions of TSSKs. The relative expression values were finally normalized to the vehicle (DMSO)-treated control and expressed as the mean ± S.D.

Protein Half-life Determination—293T cells expressing Myc-tagged kinases were pretreated for 5 min with 100 μg/ml cycloheximide and then treated with either DMSO or 1 μM 17-AAG for various time points. Cells were harvested at the given time points of incubation, and the lysates were analyzed in Western blotting with Myc and β-tubulin antibodies. Densitometry values of the TSSKs bands were divided by those of the endogenous β-tubulin and then normalized to the zero time points. The normalized values were used to calculate the half-life of TSSKs as described by Belle *et al.* (38) assuming that protein-degradation follows first-order decay kinetics.

Isolation, Enrichment, and Primary Culture of Mouse Spermatids—Mice were handled and sacrificed in accordance with the guidelines of the Animal Care and Use Committee (Center for Biologics and Evaluation Research, Food and Drug Administration). Male germ cells were isolated by enzymatic dissociation of testes from 8–12-week-old mice, and the cells were separated by sedimentation at unit gravity in 2–4% BSA gradient in a STA-PUT apparatus (ProScience Inc., GlassShop, Toronto, ON, Canada) according to the method described by La Salle *et al.* (39). After sedimentation, the fractions were examined under a microscope, and the germ cell types were identified based on size and the morphological criteria as described by Bellvé (40). Fractions containing enriched spermatocytes and spermatids were pooled separately. Average purity obtained for the enriched spermatocytes or spermatids was >90%. For the primary culture, 15 million spermatids were incubated in a 30-mm Petri dish containing 5 ml of medium (DMEM supplemented with nonessential amino acids, 5% fetal bovine serum, penicillin/streptomycin, 15 mM HEPES, 1 mM sodium pyruvate, and 6 mM sodium lactate) and treated with 10 μM HSP90 inhibitor (17-AAG, SNX-5422, or NVP-AUY922) or DMSO (vehicle) when required. Cells were incubated at 32 °C and 5% CO_2 in air and pelleted at 800 × *g* for 10 min, washed with PBS, and lysed.

Cell Viability Assay—Viability of 293T cells, COS-7 cells, and mouse spermatids was determined by trypan blue stain exclusion. At least 100 cells were counted in each field, and the average of percent viability was calculated from three such fields in an experiment. Mean percent viability from three independent experiments was calculated, and data were presented as the mean ± S.D.

Densitometry and Statistical Analysis—Western blots were scanned, and protein band intensities were quantified using Kodak MI S.E. software. For the quantification of degradation, densitometry values of TSSK bands were divided by those of endogenous β-tubulin and normalized to vehicle (DMSO)-treated samples. Normalized values from three independent experiments were used for statistical analysis, and results were expressed as the mean ± S.D. Student's *t* test was performed, and *p* values were calculated.

RESULTS

TSSKs Associate with the HSP90 Machinery—We evaluated the physical association between TSSKs and the HSP90 machinery using a co-immunoprecipitation approach and also assessed their catalytic activities *in vitro*. Myc-tagged spermatid kinases TSSK1, -2, -3, -4, or -6 were ectopically expressed in 293T cells. The kinases were immunoprecipitated from the Triton X-100 lysates, and kinase reactions were performed on the Myc immune complexes with [^{32}P]ATP and histone H2A as substrates. As shown in the autoradiogram in Fig. 1, TSSK1, -2, -4, and -6 phosphorylated histone H2A, demonstrating that the ectopically expressed kinases were catalytically active in the cells. However, TSSK3 did not have any detectable kinase activity using the H2A substrate (Fig. 1). Kinase assays testing histone H1 and myelin basic protein (MBP) as substrates also did not reveal any kinase activity associated with TSSK3 (data not shown). Furthermore, no TSSK3 autophosphorylation could be observed in the absence or presence of an exogenous protein substrate, and extensive efforts to detect TSSK3 kinase activity in lysates generated using other detergents such as pyridinium betain, 3-[(3-cholamidopropyl) dimethylammonio]-1-propanesulfonate, and *n*-dodecyl β-maltopyranoside were also not successful (data not shown). Blots containing the immune com-

plexes were probed with HSP90 antibody to evaluate the association of the kinases with HSP90 (Fig. 1). HSP90 was detected in the immune complexes of TSSK1, -2, -4, and -6, whereas the immune complexes from the empty vector control or TSSK3 did not detect HSP90, demonstrating that TSSK1, -2, -4, and -6 specifically associate with the HSP90 machinery in cells. The presence of the TSSKs and consistent amounts of endogenous HSP90 was confirmed in Western blot analysis of the lysates using Myc and HSP90 antibodies, respectively. The Myc-tagged TSSK2 migrated as a doublet with the predicted full-length protein at ~44 kDa and a smaller ~34 kDa band in SDS-PAGE (Fig. 1). Analysis of TSSK2 using NetStart 1.0 program (41) predicted an alternative translational start site at nucleotide position 181 in the cDNA sequence that may have given rise to the lower TSSK2 band observed in the blots. Alternatively, the smaller TSSK2 protein could have resulted from proteolytic cleavage of full-length TSSK2.

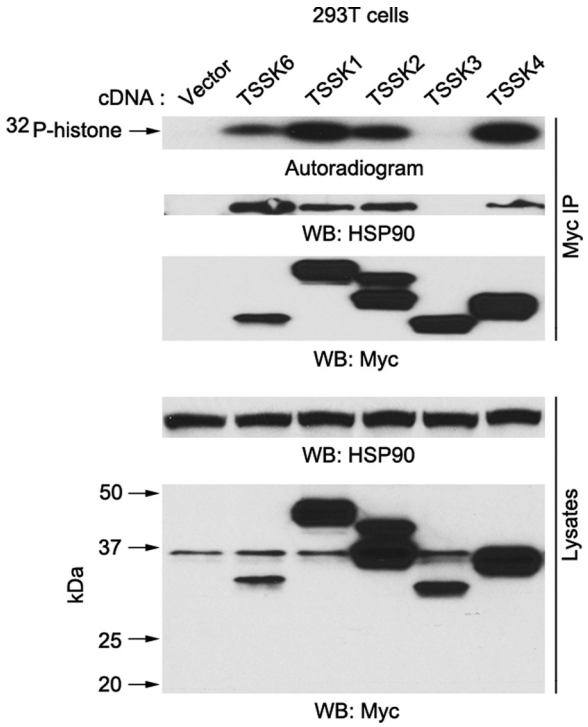

FIGURE 1. **Association with HSP90 and kinase activities of TSSKs.** cDNA constructs for the Myc-tagged kinases or the empty vector were transfected in 293T cells. Kinases were immunoprecipitated using Myc monoclonal (9E-10) antibody (*Myc IP*), and *in vitro* kinase assays were performed using [^{32}P]ATP and histone H2A as substrates. Reaction mixtures were fractionated in SDS-PAGE gels, and an autoradiogram was developed (*top*). Myc immunoprecipitates and cell lysates were analyzed in Western blotting (*WB*) with HSP90 and Myc antibodies. Positions of marker proteins and their molecular mass in kDa are indicated with *arrows*.

Inhibition of the HSP90 ATPase Results in Reduced TSSK Protein Levels in 293T Cells—Pharmacological inhibition of the HSP90 ATPase activity is known to cause degradation of many HSP90 client proteins (16, 19–21), and therefore, we next investigated the effect of HSP90 inhibition on the stability of the TSSKs. 293T cells expressing the Myc-tagged kinases were treated with HSP90 inhibitors such as 17-AAG, SNX-5422, or NVP-AUY922 (1 μM), and the cell lysates were analyzed by Western blotting with Myc antibody to measure the cellular levels of these kinases. As shown in Fig. 2*A*, treatment of cells with each of these HSP90 inhibitors caused a significant reduction in TSSK1, -2, -4, and -6 in the cells. TSSK3 protein was also reduced, albeit marginally, by treatment of cells with the drugs, and no effect was detected on the cellular levels of Myc-tagged CDK2, confirming the specificity of the effect of HSP90 inhibition on the TSSKs (Fig. 2, *A* and *B*). We determined that 17-AAG had a dose-dependent effect on the stability of TSSK1, -2, -4, and -6, with effects observed between 0.25 and 1 μM concentrations (Fig. 2*C*). Cell viability was measured, and no toxicity was found to be associated with treatment of the cells

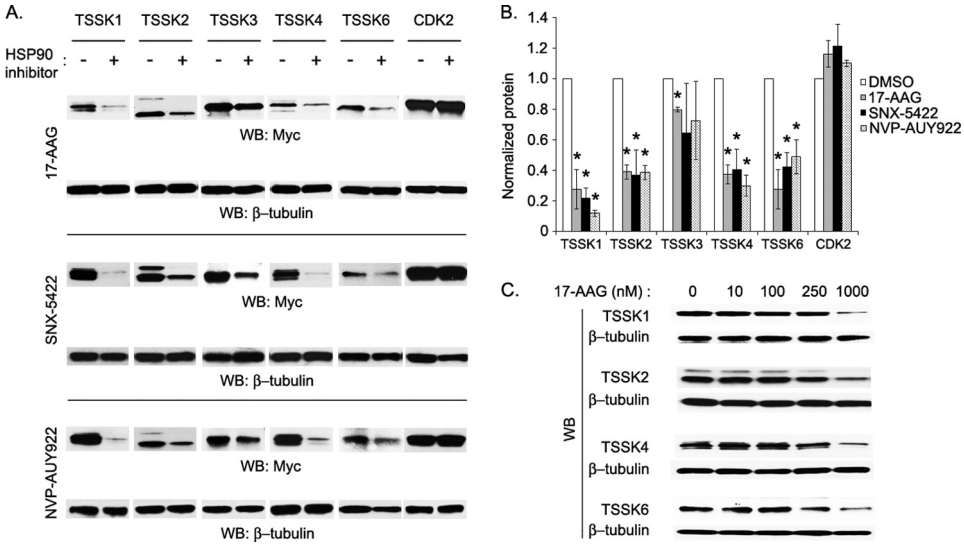

FIGURE 2. **Effects of HSP90 inhibitors on TSSK levels in 293T cells.** Myc-tagged kinases were expressed in 293T cells, and cells were treated with DMSO (vehicle) or 1 μM 17-AAG, SNX-5422, or NVP-AUY922 for 16 h. *A*, cell lysates were probed in WB with Myc or β-tubulin antibodies, and the results from a representative experiment are shown. Vehicle or HSP90 inhibitor is represented by − and + signs, respectively. *B*, shown are normalized protein levels of the kinases. TSSKs and CDK2 were analyzed as in *A*, and bands were quantified by densitometry and normalized as described under "Experimental Procedures." Values are expressed as the mean ± S.D. of three independent experiments. The *asterisk* (*) indicates that the value has a $p < 0.050$ when compared with the vehicle treated control. *C*, shown are the dose-dependent effects of 17-AAG on TSSK levels. 293T cells expressing Myc-tagged TSSK1, -2, -4, or -6 were treated for 16 h with the indicated concentrations of 17-AAG. WBs of lysates with Myc and β-tubulin antibodies from a representative experiment are shown.

with the HSP90 inhibitors at 1 μM concentration for 16 h (Table 1). Together, these data indicated that loss of HSP90 function in cells leads to a specific destabilization and reduced protein levels of the TSSK1, -2, -4, and -6.

Attenuation of HSP90 Function Leads to Accelerated TSSK Degradation in Cycloheximide-treated Cells—A reduction in the levels of steady state TSSKs could have resulted from changes in the rates of their synthesis and/or degradation. To assess the effects of attenuation of HSP90 function on the post-translational half-lives of the TSSKs, we performed a time course measurement of TSSK protein levels in 293T cells when translation was blocked with cycloheximide (Fig. 3, *A* and *B*). In the presence of cycloheximide, all of these kinases were completely lost in 16 h (data not shown). When compared with the vehicle control, the cellular levels of TSSK1, -2 and -6 were significantly reduced upon treatment with 17-AAG for 2 h, and these proteins were undetectable after 4–7 h (Fig. 3*A*). In the vehicle-treated cells the calculated half-lives of TSSK1, -2, and -6 were 1.9, 3.8, and 1.5 h, respectively, and with 17-AAG treatment, the half-lives decreased to 0.6 h for TSSK1 and TSSK2 and 0.7 h for TSSK6 (Fig. 3*B*). TSSK4 was observed to have a much shorter half-life (0.8 h) than the other TSSKs as evident by a drastic reduction in its protein level in 1 h and a complete loss within 2 h (Fig. 3*A*), and inhibition of HSP90 function did not significantly change the half-life of TSSK4 when compared with the vehicle-treated control (Fig. 3*B*). We also evaluated the degradation of TSSK4 in the presence of cycloheximide after 5-, 15-, 30-, and 60-min exposures to 17-AAG and still observed no difference in the levels of TSSK4 in control *versus* 17-AAG-treated cells (data not shown). In comparison to the other TSSKs, TSSK3 had a much longer half-life (7.4 h), and no significant difference between the drug and vehicle treatments was observed on the degradation kinetics of TSSK3 (Fig. 3, *A* and *B*) in the presence of cycloheximide. Furthermore, no significant changes in mRNA levels of TSSKs were observed after a 16-h exposure of the cells to 17-AAG (Fig. 3*C*). Together, these findings demonstrated that inhibition of HSP90 increased the rate of degradation of TSSK1, -2, and -6.

HSP90 Is Required for Activation of TSSK4 and -6 but Not TSSK1 and -2—HSP90 is known to bind partially folded client proteins including many kinases and thus influences their activation. To evaluate the role of HSP90 activity in TSSK enzymatic activation, 293T cells expressing TSSK1, -2, -4, or -6 were treated with 1 μM 17-AAG, SNX5422, NVP-AUY922, or DMSO (vehicle) for 16 h, and their kinase activities were measured as described above. Treatment of cells with the HSP90 inhibitors completely abolished the catalytic activity of TSSK4 and -6, demonstrating that HSP90 function is essential for the activation of these kinases (Fig. 4*A*). Interestingly, TSSK1 and -2 derived from the drug-treated cells possessed kinase activity, and the specific activities of these kinases were not dramatically changed. As a control, we used Myc-tagged CDK2, which was found to be insensitive to HSP90 inhibition (Fig. 4*A*). To confirm our interpretation of the findings in Fig. 4*A*, we next made a series of dilutions of TSSK1, -2, -4, and -6 control lysates and performed parallel immunoprecipitations to obtain identical amounts of the TSSKs in the immunoprecipitates from vehicle and 17-AAG-treated cell lysates. The results of head-to-head

TABLE 1

Cell viability in the presence of HSP90 inhibitors

Cells were treated with DMSO (vehicle) or the HSP90 inhibitor (1 μM for 293T and COS-7 cells and 10 μM for mouse spermatids) for 16 h, and then cell viability was measured by trypan blue exclusion. Percent cell viability is presented as mean ± S.D. from three independent experiments. ND, not determined.

Cells	DMSO	17-AAG	SNX-5422	NVP-AUY922
293T	96 ± 2	95 ± 2	94 ± 2	96 ± 3
COS-7	96 ± 3	95 ± 4	ND	ND
Spermatids	95 ± 3	94 ± 3	95 ± 2	93 ± 3

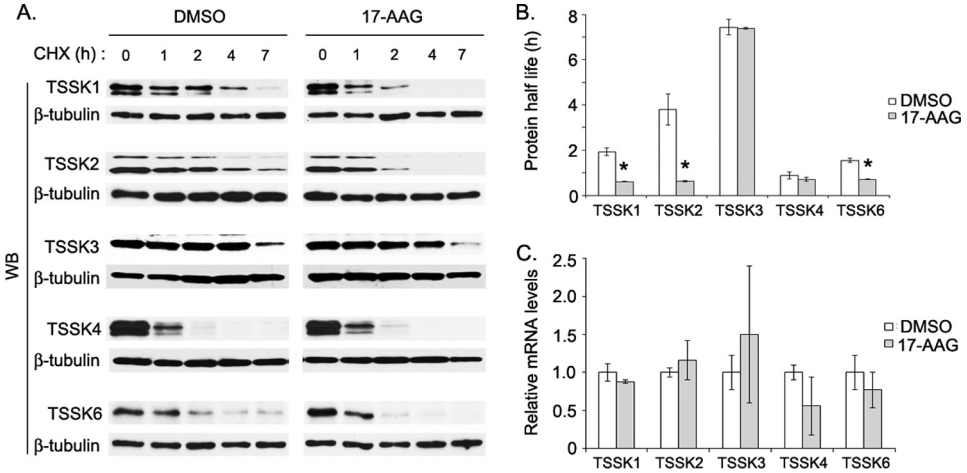

FIGURE 3. **Influence of HSP90 inhibition on the degradation of TSSK proteins and their mRNA levels.** 293T cells expressing Myc-tagged TSSKs were treated with cycloheximide (*CHX*) in the presence of either DMSO (vehicle) or 1 μM 17-AAG for the indicated time periods, and cells were lysed. *A*, lysates were evaluated by WB with Myc and β-tubulin antibodies, and the results from a representative experiment are shown. *B*, shown are half-lives of TSSKs in CHX-treated cells. TSSKs were analyzed as in *A*, and protein half-lives of TSSKs were calculated as described under "Experimental Procedures." Values are expressed as the mean ± S.D. of three independent experiments. The *asterisk* * indicates that the value has a $p < 0.050$ when compared with the vehicle-treated control. *C*, shown is measurement of mRNA levels in 17-AAG-treated 293T cells. Cells expressing Myc-tagged TSSKs were treated with either DMSO or 1 μM 17-AAG for 16 h. Total RNA was extracted and reverse-transcribed to cDNA using oligo-dT primers. Quantitative RT-PCR assays were performed using SYBR Green (Bio-Rad), and transcript levels were normalized to actin mRNA. Relative mRNA levels in the 17-AAG-treated samples were calculated with respect to the vehicle- treated samples, and values are expressed as the mean ± S.D. of triplicates. All *p* values were >0.050. This analysis was repeated three times, and the results from a representative experiment are shown.

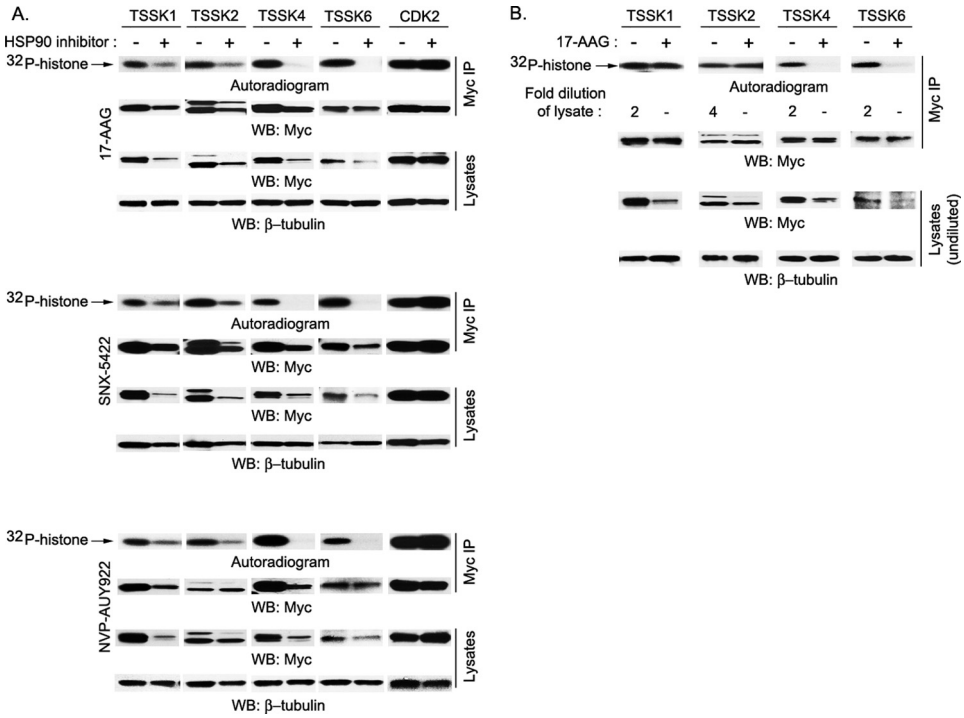

FIGURE 4. **Enzymatic activities of TSSKs in 293T cells treated with the HSP90 inhibitors.** *A*, 293T cells expressing the Myc-tagged kinases were treated with DMSO (vehicle) or 1 μM 17-AAG, SNX-5422, or NVP-AUY922 for 16 h. Myc immunoprecipitations for TSSK1, -2, -4, or -6 and CDK2 were performed, and kinase assays were carried out using [^{32}P]ATP and either histone H2A (for TSSKs) or histone H1 (for CDK2) as substrates as described in Fig. 1. Autoradiograms, WBs of the immune complexes (*Myc IP*) with Myc antibody, and blots of lysates with Myc and β-tubulin antibodies are shown from a representative experiment that was repeated three times. Vehicle or HSP90 inhibitor is represented by − and + signs, respectively. *B*, shown is a head-to-head comparison of the kinase activities associated with identical amounts of TSSKs from DMSO- and 17-AAG-treated cells. Kinase assays were performed as in *A* except that control lysate was diluted as indicated before immunoprecipitation. Immunoprecipitation of undiluted 17-AAG lysates is noted by a minus (−) sign, and analysis of undiluted lysates probed with Myc and β-tubulin antibodies is presented. Results from a representative experiment are shown.

immune complex kinase assays performed on immunoprecipitates that contained comparable amounts of each TSSK are presented in Fig. 4*B*. The findings confirmed that inhibition of HSP90 abolishes the kinase activities of TSSK4 and -6 and does not influence the kinase activities of TSSK1 and -2. As expected, the levels of the TSSKs were significantly reduced in undiluted lysates of the drug-treated cells when compared with that of the vehicle-treated controls (Fig. 4*B*). To determine whether 17-AAG treatment of cells caused a disruption of the TSSK/HSP90 complexes, we probed the Myc immune complexes in Western blotting with HSP90 antibody and found that 17-AAG did not significantly change the amounts of HSP90 detected relative to immunoprecipitated TSSK (data not shown). Furthermore, to rule out a direct inhibition of the TSSKs by the HSP90 inhibitors, we performed the kinase assays with 17-AAG added to the *in vitro* kinase reaction mix containing the immunoprecipitated kinase (TSSK1, -2, -4, or -6) and observed no effect on their catalytic activities (data not shown). These results demonstrated that HSP90 function plays a requisite role in catalytic activation of TSSK4 and -6 but not TSSK1 and -2 in cells.

HSP90 Machinery Is Necessary for the Stability and Kinase Activities of TSSKs in COS-7 Cells—We used COS-7 cells as another model to verify our findings from 293T cells. Myc-tagged TSSK1, -2, -3, -4, or -6 were ectopically expressed in COS-7 cells, and the cells were treated with 1 μM 17-AAG for 16 h. Cell viability measurements revealed no toxicity associated with 17-AAG in these cells (Table 1). The kinases were immunoprecipitated, and *in vitro* kinase reactions were performed on the Myc immune complexes as described above. HSP90 inhibition in COS-7 cells completely abolished the catalytic activities of TSSK4 and -6, indicating that the HSP90 function is essential for their activation (Fig. 5*A*). Immunoprecipitates containing either TSSK1 or -2 from 17-AAG-treated cells had reduced kinase activities compared with the vehicle control, but the specific activities of the kinases was not significantly altered (Fig. 5*A*). Again, we did not observe any kinase activity in the TSSK3 immunoprecipitates. Similar to the 293T cell findings, these results demonstrated that HSP90 function is essential for catalytic activation of TSSK4 and -6 but not TSSK1 and -2. However, unlike our findings in 293T cells, treatment of COS-7 cells with 17-AAG caused a disruption of the complex of TSSK1, -2, -4, or -6 with HSP90 as indicated by the complete loss of HSP90 in the Western blots of the Myc immune complexes (data not shown). Western blotting analysis of the lysates demonstrated that attenuation of HSP90 function caused a significant reduction in protein levels of the TSSKs in COS-7 cells (Fig. 5, *A* and *B*). Neither the kinase activity nor stability of Myc-tagged CDK2 was affected by treatment of cells with 17-AAG, confirming the specificity of the effect on the TSSKs. As was done for 293T lysates, we diluted control lysate before immunoprecipitation to achieve identical amounts of the immunoprecipitated TSSKs from lysates of vehicle- and 17-AAG-treated cells and performed the kinase reactions (Fig. 5*C*). These results confirmed that HSP90 is required for the catalytic activities of TSSK4 and -6 but not for TSSK1 and -2.

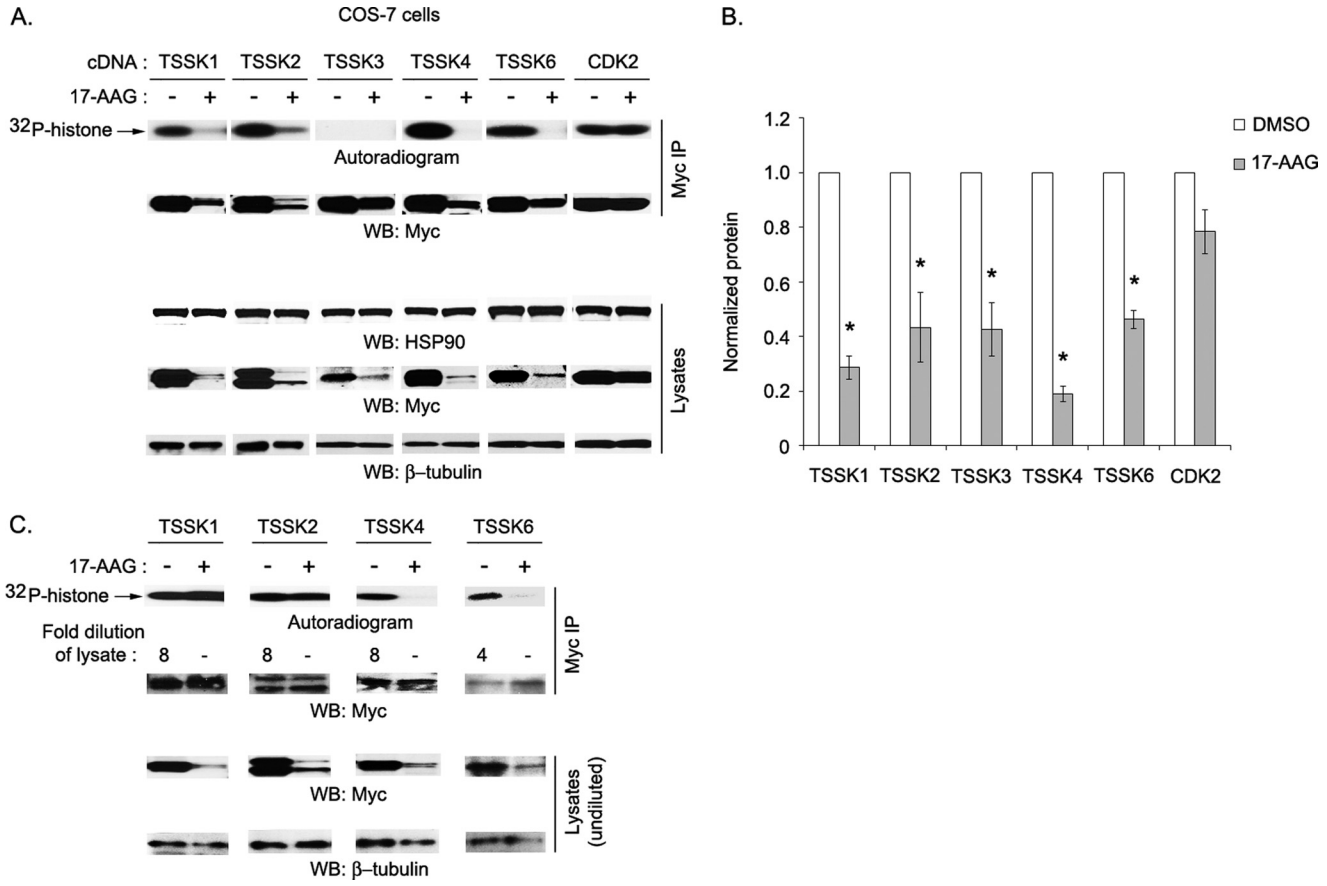

FIGURE 5. **Effect of 17-AAG on enzymatic activities and stability of TSSKs in COS-7 cells.** Myc-tagged kinases were expressed in COS-7 cells, and cells were treated with 1 μM 17-AAG or DMSO (vehicle) for 16 h. Myc immunoprecipitations for TSSKs and CDK2 were performed, and kinase assays were carried out using [^{32}P]ATP and histone as substrates as described in Fig. 4. *A*, autoradiograms and WBs of the Myc antibody immune complexes (*Myc IP*), and blots of lysates with HSP90, Myc, and β-tubulin antibodies are shown from a representative experiment that was repeated three times. Vehicle or 17-AAG is represented by $-$ and $+$ signs, respectively. *B*, normalized TSSK protein levels are shown. TSSKs and CDK2 levels in lysates were analyzed as in *A*, and protein bands were quantified by densitometry and normalized as described under "Experimental Procedures." Values are expressed as the mean $\pm$ S.D. of three independent experiments. The asterisk (*) indicates a $p < 0.050$ when compared with the vehicle-treated control. *C*, shown is a comparison of the kinase activities associated with identical amounts of TSSKs from DMSO- and 17-AAG-treated COS-7 cells. Kinase assays were performed as in *A* except that control lysate was diluted as indicated before immunoprecipitation. Immunoprecipitation of undiluted 17-AAG lysates is noted by a minus ($-$) sign, and analysis of undiluted lysates probed with Myc and β-tubulin antibodies is presented.

HSP90 Inhibition Increases TSSK Ubiquitination and Degradation via the Proteasome—To better understand the mechanism for HSP90-mediated stabilization of the TSSKs in cells, we first tested whether HSP90 inhibition leads to TSSK degradation by the proteasome pathway. COS-7 cells expressing Myc-tagged TSSKs were treated with the highly specific proteasomal inhibitors MG132 (5 μM) or epoxomicin (0.2 μM) for 16 h in the presence or absence of 1 μM 17-AAG, and the cell lysates were analyzed by Western blotting with Myc and β-tubulin antibodies. As shown in Fig. 6, treatment of control cells (no 17-AAG) with MG132 (*left*) or epoxomicin (*right*) slightly increased the cellular levels of the TSSK1, -3, and -6, relative to tubulin. Importantly, the 17-AAG-induced decreases in cellular levels of TSSK1, -2, -3, -4, and -6 were dramatically blocked by the proteasomal inhibitors, demonstrating that HSP90 inhibition leads to the degradation of these TSSKs by the proteasome (Fig. 6). Similar results were obtained in 293T cells using MG132 and epoxomicin (data not shown).

We next examined whether TSSKs are subjected to ubiquitination in cells. Myc-tagged TSSKs and HA-tagged ubiquitin were co-expressed in COS-7 cells, lysed in non-denaturing

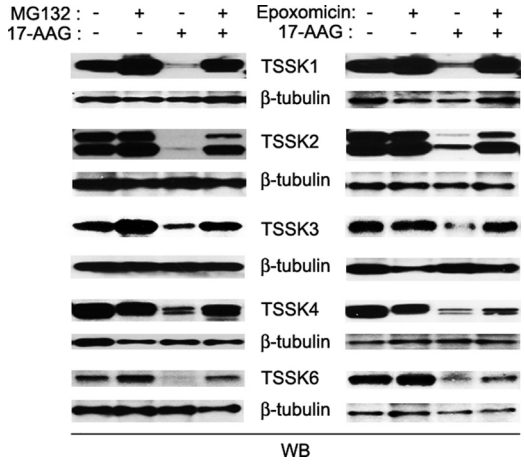

FIGURE 6. **Influence of proteasomal inhibitors on 17-AAG induced degradation of TSSKs.** COS-7 cells expressing Myc-tagged TSSKs were incubated with DMSO (vehicle) or the proteasomal inhibitor (5 μM MG132 or 0.2 μM epoxomicin) either in the presence or absence of 1 μM 17-AAG for 16 h. Cell lysates were evaluated by WB with Myc and β-tubulin antibodies, and results from a representative experiment are shown. Vehicle is represented by a $-$ sign, and either 17-AAG or MG132 is represented by a $+$ sign.

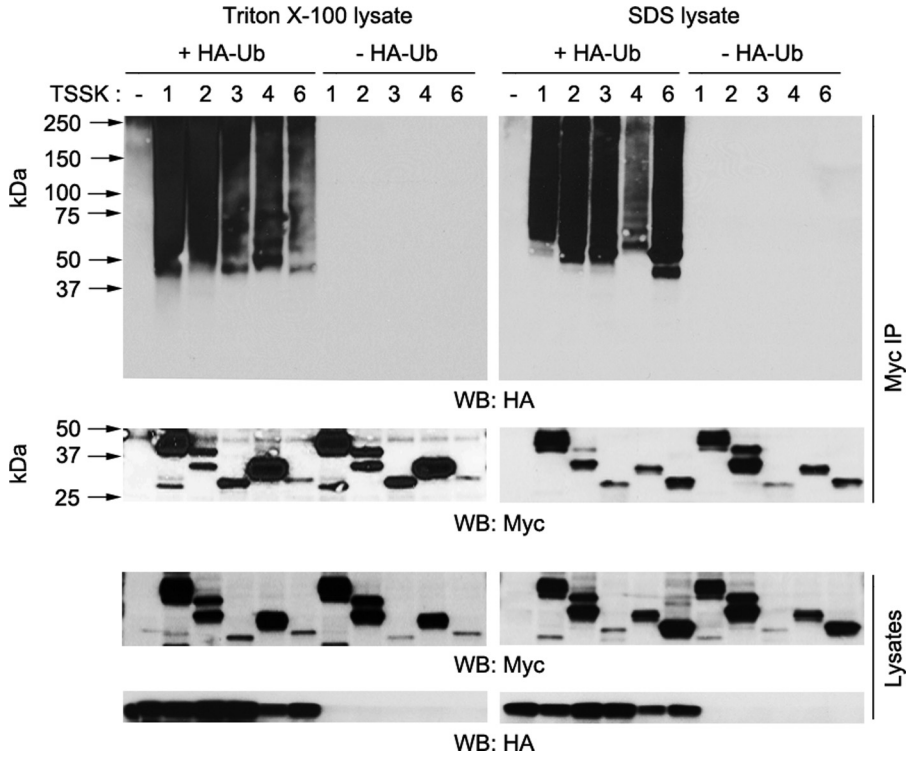

FIGURE 7. **Ubiquitination of TSSKs.** A Myc-tagged cDNA construct for each TSSK or empty vector (−) was transfected in COS-7 cells either alone or with cDNA encoding HA-tagged ubiquitin (*HA-Ub*). Total cell proteins were extracted either in non-denaturing buffer (Triton X-100; *left panels*) or in denaturing buffer (SDS; *right panels*), and Myc immunoprecipitations were performed. Protein extracts in SDS buffer were denatured by boiling, and lysate was diluted 10-fold with Nonidet P-40 buffer before the immunoprecipitation. WB of Myc immunoprecipitates and cell lysates probed with HA and Myc antibodies from a representative experiment are shown. Positions of marker proteins and their molecular mass in kDa are indicated with *arrows*.

buffer (Triton X-100), and immunoprecipitated with Myc antibody. Ubiquitination of TSSKs was assessed in Western blotting of the Myc immunoprecipitates with HA antibody. As shown in Fig. 7, *left top panel*, an HA immunoreactive high molecular mass ladder of bands was observed in the immunoprecipitates derived from cells co-transfected with Myc-TSSK and HA-ubiquitin cDNAs but not from control cells transfected with either cDNA alone, demonstrating that the TSSKs were ubiquitinated. The HA-reactive ladder of bands migrated above the unmodified TSSKs. To test whether ubiquitin was directly linked to TSSKs and not co-immunoprecipitated via non-covalent interactions, we extracted and denatured the proteins by boiling in SDS buffer followed by dilution with non-denaturing (Nonidet P-40) buffer and immunoprecipitation of TSSKs with Myc antibody. The HA-reactive high molecular mass ladder of bands was again present in the Myc-immunoprecipitates, demonstrating that ubiquitin was directly conjugated to TSSKs (Fig. 7, *right top panel*). Western blot analysis with Myc and HA antibodies confirmed the presence of TSSKs in the immunoprecipitates and expression of HA-ubiquitin and TSSKs in cells (Fig. 7). To evaluate the influence of HSP90 function on TSSK ubiquitination, cells expressing Myc-TSSK1, -2, -3, -4, or -6 and HA-ubiquitin were simultaneously treated with 17-AAG and MG132. Ubiquitination of TSSKs was assessed in Western blotting of the Myc-immunoprecipitates with HA antibody. Exposure of cells to 17-AAG increased the levels of ubiquitination for each TSSK when compared with the control (no 17-AAG), demonstrating that HSP90 inhibition leads to enhanced ubiquitination of TSSKs (Fig. 8). Collectively, these

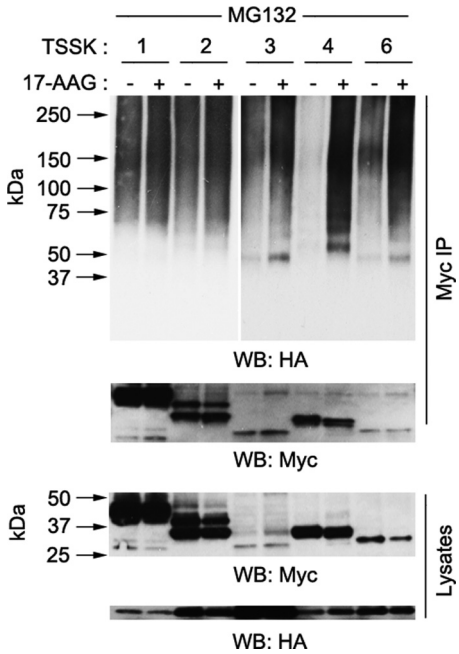

FIGURE 8. **Effects of attenuation of HSP90 function on TSSKs ubiquitination.** Myc-tagged TSSKs and HA-tagged ubiquitin (HA-Ub) were co-expressed in COS-7 cells, and cells were treated for 8 h with 5 μM MG132 in the absence (DMSO, vehicle) or presence of 1 μM 17-AAG. Vehicle or 17-AAG is represented by − and + signs, respectively. Ubiquitination was analyzed by Western blotting (WB) of the Myc immunoprecipitates (*Myc IP*) using HA and Myc antibodies, and cell lysates were probed with HA and Myc antibodies. Results are shown from a representative experiment that was repeated three times. Positions of marker proteins and their molecular mass in kDa are indicated with *arrows*.

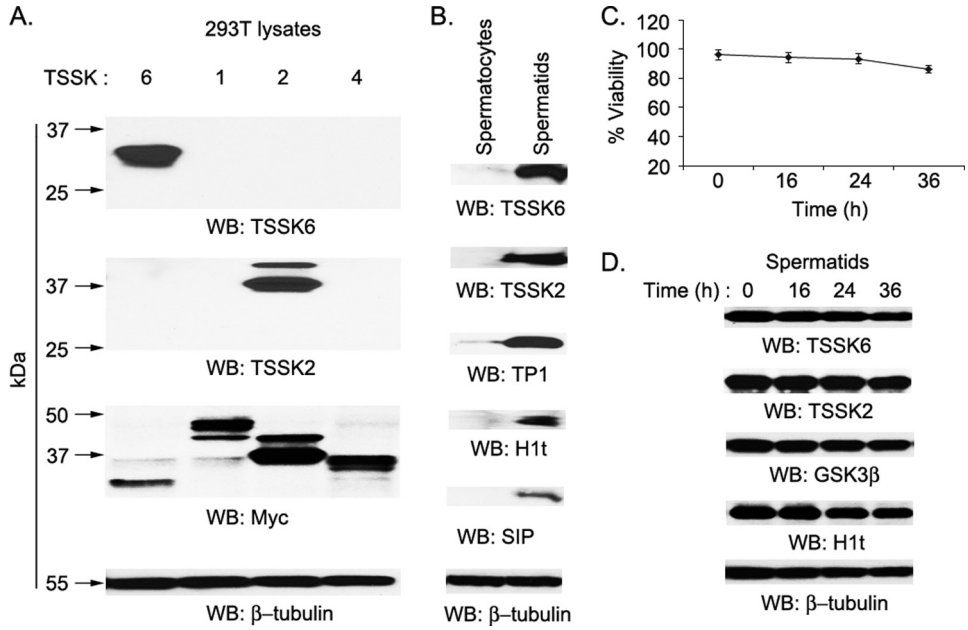

FIGURE 9. **Isolation and characterization of spermatids from mouse testes.** *A*, validation of TSSK antibodies is shown. Lysates of 293T cells expressing Myc-tagged TSSK1, -2, -4, or -6 were probed in WB with TSSK6, TSSK2, Myc, and β-tubulin antibodies. Molecular masses in kDa are marked with *arrows*. *B*, shown is characterization of mouse male germ cells. Enriched populations of mouse spermatocytes and spermatids were purified by cellular sedimentation in a STA-PUT apparatus. WB was performed with TSSK2, TSSK6, transition protein 1 (*TP1*), H1t, small serine/threonine kinase (SSTK)-interacting protein (SIP), and β-tubulin antibodies. *C*, enriched spermatid populations were cultured *in vitro*, and cell viability was measured by trypan blue exclusion at the indicated times. Values are presented as the mean ± S.D. ($n = 3$). *D*, enriched spermatids populations were incubated for various time periods, and lysates were analyzed in WB with TSSK6, TSSK2, GSK3β, H1t, and β-tubulin antibodies.

data demonstrated that TSSKs are ubiquitinated and HSP90 functions to regulate the ubiquitination of TSSKs in cells.

Inhibition of HSP90 Results in Decreased TSSK2 and -6 in Mouse Spermatids—We developed a primary spermatid culture model to evaluate the effects of HSP90 inhibition on endogenous TSSKs in mouse germ cells. To assess the stability and kinase activities of TSSKs from mouse spermatids, we obtained antibodies for the individual TSSKs and characterized them for specificity and cross-reactivity in Western blotting of lysates from 293T cells expressing Myc-tagged TSSKs. An in-house monoclonal TSSK6 antibody was used (33) and antibodies for TSSK1, -2, and -4 were obtained from commercial sources. Among all the antibodies for TSSKs that we tested, only the TSSK2 and -6 monoclonal antibodies had adequate sensitivity and were highly specific as evident by the finding that these two antibodies did not cross-react with other TSSK family members (Fig. 9*A*). Next, we characterized the TSSK2 and -6 antibodies for their utility in immune complex kinase assays. Although both antibodies immunoprecipitated their respective TSSK, only the immune complexes that contained murine TSSK2 had detectable specific kinase activity (data not shown). As for the TSSK6 immunoprecipitates, the lack of detectable kinase activity was presumably due to inactivation of TSSK6 as the antibody is directed against the kinase domain (33). Efforts to confirm the association of endogenous TSSK2 and -6 with HSP90 in spermatids by co-immunoprecipitation were unsuccessful (data not shown).

To further assess HSP90 function in germ cells, we developed and characterized a primary spermatid culture derived from mouse testes. Enriched populations of spermatocytes and spermatids were obtained from the testes of adult mice (8–12 weeks old) by cellular sedimentation in a BSA gradient using a STA-PUT apparatus. The enrichment of the spermatocytes and the spermatids was confirmed by examining the cells under a microscope, and the germ cell types were identified based on size and the morphological criteria as described by Bellvé (40). Furthermore, Western blotting analysis of the cell lysates with specific antibodies against spermatid-specific proteins such as TSSK2, TSSK6, transition protein 1 (*TP1*), testis-specific H1t, and SIP (TSACC) confirmed that a highly enriched population of spermatids was obtained using this methodology (Fig. 9*B*). 15 million cells from the enriched spermatid pool were cultured in medium under sterile conditions at 32 °C and 5% CO_2. Percent cell viability of spermatids in the culture was maintained at ~93% for 24 h and at ~86% for 36 h of incubation (Fig. 9*C*). Cells were counted at various time points during the incubation, and the total cell number did not change in the cultures. Western blot analysis demonstrated that the levels of various germ cell proteins such as TSSK2, TSSK6, GSK3β, and H1t were stable during the culture period (Fig. 9*D*).

To evaluate the effect of HSP90 inhibition on the stability of endogenous TSSK2 and -6, the mouse spermatids were cultured and treated with 17-AAG, SNX-5422, or NVP-AUY922 (all at 10 μM) or DMSO (vehicle control) for 16 h. Cell viability was not affected by treatment with the HSP90 inhibitors (Table 1). Conversely, Western blotting analysis of lysates from spermatids treated with the HSP90 inhibitors for 16 h demonstrated that the cellular levels of TSSK2 and -6 were significantly reduced upon HSP90 inhibition (Fig. 10, *A* and *B*). The levels of endogenous GSK3β or H1t did not change (Fig. 10*A*), indicating that treatment of spermatids with the HSP90 drugs had a specific effect on the TSSKs. 17-AAG treatments of spermatids

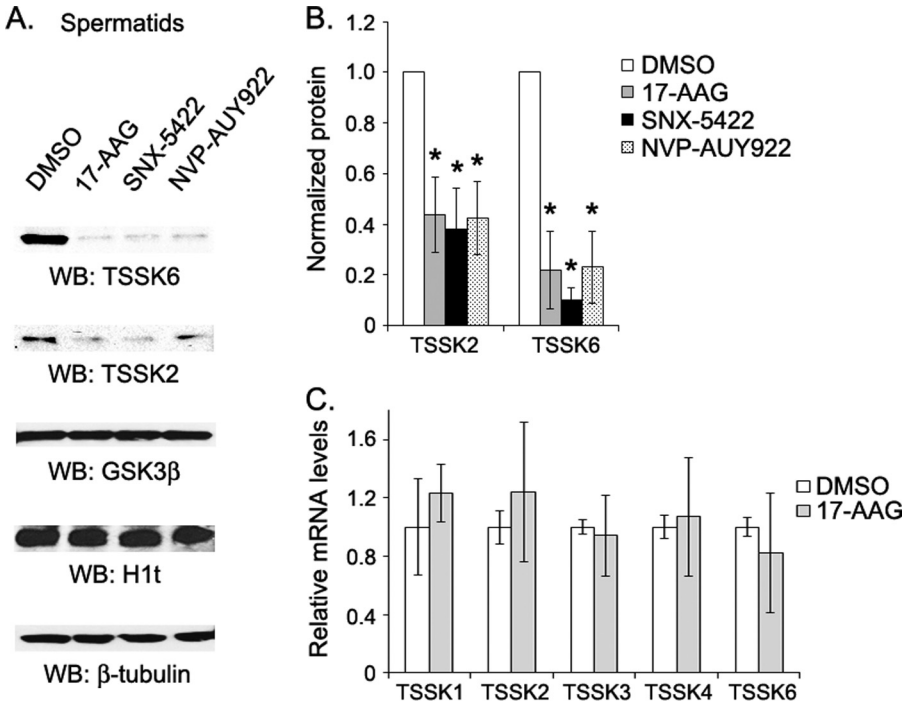

FIGURE 10. **Stability of TSSK2 and -6 in HSP90-inhibited spermatids.** *A*, enriched populations of mouse spermatids were cultured under sterile conditions at 32 °C and 5% CO_2 for 16 h and treated with either DMSO (vehicle) or 10 μM HSP90 inhibitors. Lysates were probed in WB using TSSK2, TSSK6, GSK3β, H1t, and β-tubulin antibodies. WB from a representative experiment are shown. *B*, shown are normalized TSSK2 and -6 protein levels. TSSK2 and -6 bands were quantified by densitometry and normalized as described under "Experimental Procedures." Values are expressed as the mean ± S.D. of three independent experiments. The *asterisk* (*) indicates that the value has a $p < 0.050$ when compared with the vehicle-treated control. *C*, shown are mRNA levels of TSSKs in 17-AAG-treated spermatids. Total RNA was extracted from the spermatids treated with either DMSO or 17-AAG and reverse-transcribed to cDNA using oligo-dT primers. Quantitative RT-PCR assays were performed using SYBR Green (Bio-Rad), and transcript levels were normalized to actin mRNA. Relative mRNA levels in the 17-AAG-treated samples were calculated with respect to the vehicle-treated samples, and values are expressed as the mean ± S.D. of triplicates. All *p* values were >0.050.

did not alter the mRNA levels of TSSKs (Fig. 10*C*). As expected, the kinase activity in TSSK2 immunoprecipitates from spermatids treated with HSP90 inhibitors was reduced relative to vehicle-treated cells, and consistent with the findings from 293T and COS-7 cells, the specific activity of TSSK2 was unchanged (data not shown). In conclusion, these results demonstrated that inhibition of HSP90 leads to a striking decrease of endogenous TSSK2 and -6 proteins in living germ cells.

DISCUSSION

The TSSKs are expressed exclusively in the post-meiotic male germ cells of mammals, are essential for male fertility, and play important roles in spermatid development and/or sperm function (9–11, 13). In the present study we have explored the role of HSP90 function in the stabilization and catalytic activation of all TSSK family members using ectopically expressed epitope-tagged TSSKs in 293T and COS-7 cells. We have also investigated the mechanism of how HSP90 stabilizes the TSSKs and the impact of ubiquitination and the proteasome in this process. Finally, to evaluate the ability of HSP90 to regulate TSSKs in male germ cells, we have developed a primary spermatid culture and utilized this novel model system to study the effects of pharmacological inhibition of HSP90 on the TSSKs.

HSP90 is a ubiquitously expressed protein that is involved in native folding, stabilization, maturation, and activation of numerous cellular proteins (14, 15, 20). Several natural products as well as synthetic compounds inhibit HSP90 function by occupying its ATP binding pocket (21) and lead to destabilization of the client proteins including kinases, transcription factors, steroid receptors, and others such as the fibrosis transmembrane conductance regulator and huntingtin (19, 21, 24–32). Here, we used three structurally unrelated and highly selective HSP90 inhibitors, namely 17-AAG, SNX-5422, and NVP-AUY922, to evaluate the influence of HSP90 function on the stability and catalytic activities of TSSKs. We observed a specific association of TSSK1, -2, -4, and -6 with HSP90, indicating that all of these TSSKs form stable complexes with HSP90. Treatment of cells with 17-AAG blocked the co-immunoprecipitation of HSP90 with the TSSKs in COS-7 cells but not in 293T cells (data not shown). The basis for this may be due to differences in the complement of HSP90 machinery accessory proteins and co-chaperones and/or differential cycling rates for the TSSK/HSP90 complexes in the two cell lines. Importantly, pharmacological inhibition of the HSP90 ATPase elicited a consistent reduction in the cellular protein levels of these TSSKs in both 293T and COS-7 cells without altering their mRNA levels. Further analysis demonstrated that treatment with the HSP90 inhibitors resulted in the accelerated degradation of TSSK1, -2, and -6 in cycloheximide-treated cells and reduced their post-translational half-lives. However, an increased rate for TSSK4 degradation by 17-AAG could not be demonstrated when translation was blocked presumably because the basal degradation (no 17-AAG) was too fast (half-life of <1 h) relative to the time necessary to enhance TSSK4 degradation via HSP90 inhibition. Finally, using specific anti-

bodies, we confirmed that HSP90 inhibition resulted in degradation of endogenous TSSK2 and -6 in mouse spermatids. Our results demonstrate that HSP90 plays an important role in stabilization of TSSKs in cells.

The ubiquitin-proteasome pathway is a key mechanism regulating cellular proteins including many HSP90 clients and involves covalent attachment of ubiquitin molecules to the target proteins followed by their delivery to the proteasome and proteolytic degradation (42, 43). Attenuation of cellular HSP90 activity enhanced TSSK ubiquitination and degradation by the proteasome, indicating that HSP90 acts to control ubiquitination of TSSKs. It seems likely that when TSSKs are bound to the HSP90 machinery and undergoing HSP90-mediated conformational maturation, the ubiquitinating enzymes do not have access to the kinases. Conversely, during HSP90 ATPase inhibition and stalling of the cycling of the HSP90 machinery, ubiquitination-prone TSSK molecules may accumulate and become ubiquitinated and degraded by the proteasome. In addition to regulating the normal turnover of the TSSKs, HSP90 may also prevent any aberrant ubiquitination and degradation of the TSSKs that could occur in response to altered cellular stress conditions. Thus, we would propose that HSP90 functions as a regulator of TSSKs that can modulate TSSK protein levels depending on the needs of the differentiating germ cell.

We also evaluated the role of HSP90 in activation of TSSKs, and the results demonstrated that HSP90 function is required for the catalytic activation of TSSK4 and -6 but not for TSSK1 or -2. Hence, various TSSK family members differ from one another in terms of an HSP90 requirement for their enzyme activation, and this may be due to inherent differences in their primary structures. For example, the long C-terminal extensions in TSSK1 and -2 may facilitate the folding and generation of the active structure of the kinases, whereas association with HSP90 may be critical for the maintenance, stability, and turnover of these active conformers. In the case of TSSK4 and -6, the C-terminal extension is much shorter, and therefore, it is likely that association with HSP90 is required for their proper folding, activation, and stabilization. A recent paper provides evidence that HSP90 does not recognize specific sequence motifs in client kinases, but interacts with intrinsically unstable kinases (44). Co-chaperones play an integral role in the specificity of HSP90 for client proteins. Recently, we reported the identification and characterization of the HSP70 binding co-chaperone SIP/TSACC that is expressed exclusively in spermatids (33). SIP binds to TSSK6 and facilitates the HSP90-mediated activation of TSSK6. Our studies indicate that SIP does not associate with the other TSSKs and co-expression of SIP in cells does not result in their enzymatic activation.[4] Thus, SIP appears to be involved in the selective activation of TSSK6, and it is likely that there are undiscovered spermatid co-chaperones that function to specifically regulate the other TSSKs.

In contrast to the other TSSKs, the role of TSSK3 in spermatogenesis is not very clear and is somewhat controversial. TSSK3 protein could not be detected in testis or sperm by Western blotting or immunofluorescence, although the TSSK3 mRNA was detected (9). It was proposed that TSSK3 protein may only exist transiently *in vivo* and, thus, is not readily detected (9). In the present work TSSK3 did not co-immunoprecipitate with HSP90 in either 293T or COS-7 cells. However, TSSK3 was ubiquitinated and degraded in response to HSP90 inhibition in COS-7 cells, whereas the HSP90 inhibitors had only a modest effect on TSSK3 stability in 293T cells. No TSSK3 catalytic activity was observed in either cell line even though we made extensive experimental efforts to detect the kinase activity. TSSK3 contains all the necessary subdomains and key catalytic residues that would support a prediction that it is a functional kinase, and Bucko-Justyna *et al.* (45) reported to have measured TSSK3 catalytic activity. In any event, relative to the other TSSK family members, TSSK3 appears to be unique and may only exist as a catalytically competent enzyme under certain conditions.

Taken together, our findings indicate that HSP90 plays a broad and critical role in stabilization and activation of the TSSKs. The members of this family of protein kinases consist solely of a catalytic domain with relatively short extensions and no other protein domains. This common structure may have rendered the kinases inherently unstable and evolutionarily resulted in a requirement for HSP90 in their stability and activity. We propose that HSP90 recognizes an "HSP90-susceptible conformation" (44) in the TSSKs and cycles to stabilize the kinases. In the absence of this constant sampling and stabilization by HSP90, the kinases are targeted for ubiquitination and degradation. The male germ cells in HSP90α null mice do not progress through meiosis (34), and based upon our work reported here, it appears likely that HSP90 is also critical to spermiogenesis, the differentiation of spermatids into mature spermatozoa. It is very possible that during the post-meiotic differentiation of male germ cells, HSP90 functions to coordinate the temporal and spatial activation of the TSSKs. This may represent an efficient mechanism for the regulation and action of these kinases. Interestingly, HSP90α protein is significantly lost during the epididymal passage of spermatozoa (46) and, thus, may have a reduced role or no longer be required for function in mature sperm.

Acknowledgments—We are grateful to Dr. Avin Lalmansingh for assistance with quantitative RT-PCR and Dr. Yetao Jin for helpful discussion.

[4] K. N. Jha, A. R. Coleman, L. Wong, A. M. Salicioni, E. Howcroft, and G. R. Johnson, unpublished data.

REFERENCES

1. Cheng, C. Y., and Mruk, D. D. (2002) Cell junction dynamics in the testis. Sertoli-germ cell interactions and male contraceptive development. *Physiol. Rev.* **82,** 825–874
2. Griswold, M. D. (1995) Interactions between germ cells and Sertoli cells in the testis. *Biol. Reprod.* **52,** 211–216
3. Eddy, E. M., and O'Brien, D. A. (1998) Gene expression during mammalian meiosis. *Curr. Top. Dev. Biol.* **37,** 141–200
4. Kierszenbaum, A. L., and Tres, L. L. (1975) Structural and transcriptional features of the mouse spermatid genome. *J. Cell Biol.* **65,** 258–270
5. Ogurtsov, A. Y., Mariño-Ramírez, L., Johnson, G. R., Landsman, D., Shabalina, S. A., and Spiridonov, N. A. (2008) Expression patterns of protein kinases correlate with gene architecture and evolutionary rates. *PLoS ONE* **3,** e3599
6. Escalier, D., Silvius, D., and Xu, X. (2003) Spermatogenesis of mice lacking

CK2α′. Failure of germ cell survival and characteristic modifications of the spermatid nucleus. *Mol. Reprod. Dev.* **66,** 190–201
7. Ortega, S., Prieto, I., Odajima, J., Martín, A., Dubus, P., Sotillo, R., Barbero, J. L., Malumbres, M., and Barbacid, M. (2003) Cyclin-dependent kinase 2 is essential for meiosis but not for mitotic cell division in mice. *Nat. Genet.* **35,** 25–31
8. Wu, J. Y., Ribar, T. J., Cummings, D. E., Burton, K. A., McKnight, G. S., and Means, A. R. (2000) Spermiogenesis and exchange of basic nuclear proteins are impaired in male germ cells lacking Camk4. *Nat. Genet.* **25,** 448–452
9. Li, Y., Sosnik, J., Brassard, L., Reese, M., Spiridonov, N. A., Bates, T. C., Johnson, G. R., Anguita, J., Visconti, P. E., and Salicioni, A. M. (2011) Expression and localization of five members of the testis-specific serine kinase (Tssk) family in mouse and human sperm and testis. *Mol. Hum. Reprod.* **17,** 42–56
10. Shang, P., Baarends, W. M., Hoogerbrugge, J., Ooms, M. P., van Cappellen, W. A., de Jong, A. A., Dohle, G. R., van Eenennaam, H., Gossen, J. A., and Grootegoed, J. A. (2010) Functional transformation of the chromatoid body in mouse spermatids requires testis-specific serine/threonine kinases. *J. Cell Sci.* **123,** 331–339
11. Spiridonov, N. A., Wong, L., Zerfas, P. M., Starost, M. F., Pack, S. D., Paweletz, C. P., and Johnson, G. R. (2005) Identification and characterization of SSTK, a serine/threonine protein kinase essential for male fertility. *Mol. Cell. Biol.* **25,** 4250–4261
12. Xu, B., Hao, Z., Jha, K. N., Zhang, Z., Urekar, C., Digilio, L., Pulido, S., Strauss, J. F., 3rd, Flickinger, C. J., and Herr, J. C. (2008) Targeted deletion of Tssk1 and -2 causes male infertility due to haploinsufficiency. *Dev. Biol.* **319,** 211–222
13. Sosnik, J., Miranda, P. V., Spiridonov, N. A., Yoon, S. Y., Fissore, R. A., Johnson, G. R., and Visconti, P. E. (2009) Tssk6 is required for Izumo relocalization and gamete fusion in the mouse. *J. Cell Sci.* **122,** 2741–2749
14. Pratt, W. B., and Toft, D. O. (2003) Regulation of signaling protein function and trafficking by the hsp90/hsp70-based chaperone machinery. *Exp. Biol. Med.* (*Maywood*) **228,** 111–133
15. Wandinger, S. K., Richter, K., and Buchner, J. (2008) The Hsp90 chaperone machinery. *J. Biol. Chem.* **283,** 18473–18477
16. Waza, M., Adachi, H., Katsuno, M., Minamiyama, M., Sang, C., Tanaka, F., Inukai, A., Doyu, M., and Sobue, G. (2005) 17-AAG, an Hsp90 inhibitor, ameliorates polyglutamine-mediated motor neuron degeneration. *Nat. Med.* **11,** 1088–1095
17. Young, J. C., Moarefi, I., and Hartl, F. U. (2001) Hsp90. A specialized but essential protein-folding tool. *J. Cell Biol.* **154,** 267–273
18. Panaretou, B., Prodromou, C., Roe, S. M., O'Brien, R., Ladbury, J. E., Piper, P. W., and Pearl, L. H. (1998) ATP binding and hydrolysis are essential to the function of the Hsp90 molecular chaperone *in vivo*. *EMBO J.* **17,** 4829–4836
19. Baldo, B., Weiss, A., Parker, C. N., Bibel, M., Paganetti, P., and Kaupmann, K. (2012) A screen for enhancers of clearance identifies huntingtin as a heat shock protein 90 (Hsp90) client protein. *J. Biol. Chem.* **287,** 1406–1414
20. Marubayashi, S., Koppikar, P., Taldone, T., Abdel-Wahab, O., West, N., Bhagwat, N., Caldas-Lopes, E., Ross, K. N., Gönen, M., Gozman, A., Ahn, J. H., Rodina, A., Ouerfelli, O., Yang, G., Hedvat, C., Bradner, J. E., Chiosis, G., and Levine, R. L. (2010) HSP90 is a therapeutic target in JAK2-dependent myeloproliferative neoplasms in mice and humans. *J. Clin. Invest.* **120,** 3578–3593
21. Basso, A. D., Solit, D. B., Chiosis, G., Giri, B., Tsichlis, P., and Rosen, N. (2002) Akt forms an intracellular complex with heat shock protein 90 (Hsp90) and Cdc37 and is destabilized by inhibitors of Hsp90 function. *J. Biol. Chem.* **277,** 39858–39866
22. Rajan, A., Carter, C. A., Kelly, R. J., Gutierrez, M., Kummar, S., Szabo, E., Yancey, M. A., Ji, J., Mannargudi, B., Woo, S., Spencer, S., Figg, W. D., and Giaccone, G. (2012) A phase I combination study of olaparib with cisplatin and gemcitabine in adults with solid tumors. *Clin. Cancer Res.* **18,** 2344–2351
23. Chandarlapaty, S., Sawai, A., Ye, Q., Scott, A., Silinski, M., Huang, K., Fadden, P., Partdrige, J., Hall, S., Steed, P., Norton, L., Rosen, N., and Solit, D. B. (2008) SNX2112, a synthetic heat shock protein 90 inhibitor, has potent antitumor activity against HER kinase-dependent cancers. *Clin. Cancer Res.* **14,** 240–248
24. Schulte, T. W., Blagosklonny, M. V., Ingui, C., and Neckers, L. (1995) Disruption of the Raf-1-Hsp90 molecular complex results in destabilization of Raf-1 and loss of Raf-1-Ras association. *J. Biol. Chem.* **270,** 24585–24588
25. Tikhomirov, O., and Carpenter, G. (2000) Geldanamycin induces ErbB-2 degradation by proteolytic fragmentation. *J. Biol. Chem.* **275,** 26625–26631
26. An, W. G., Schulte, T. W., and Neckers, L. M. (2000) The heat shock protein 90 antagonist geldanamycin alters chaperone association with p210bcr-abl and v-src proteins before their degradation by the proteasome. *Cell Growth Diff.* **11,** 355–360
27. Lewis, J., Devin, A., Miller, A., Lin, Y., Rodriguez, Y., Neckers, L., and Liu, Z. G. (2000) Disruption of hsp90 function results in degradation of the death domain kinase, receptor-interacting protein (RIP), and blockage of tumor necrosis factor-induced nuclear factor-κB activation. *J. Biol. Chem.* **275,** 10519–10526
28. Blagosklonny, M. V., Toretsky, J., and Neckers, L. (1995) Geldanamycin selectively destabilizes and conformationally alters mutated p53. *Oncogene* **11,** 933–939
29. Ehrlich, E. S., Wang, T., Luo, K., Xiao, Z., Niewiadomska, A. M., Martinez, T., Xu, W., Neckers, L., and Yu, X. F. (2009) Regulation of Hsp90 client proteins by a Cullin5-RING E3 ubiquitin ligase. *Proc. Natl. Acad. Sci. U.S.A.* **106,** 20330–20335
30. Faresse, N., Ruffieux-Daidie, D., Salamin, M., Gomez-Sanchez, C. E., and Staub, O. (2010) Mineralocorticoid receptor degradation is promoted by Hsp90 inhibition and the ubiquitin-protein ligase CHIP. *Am. J. Physiol. Renal Physiol.* **299,** F1462–F1472
31. Segnitz, B., and Gehring, U. (1997) The function of steroid hormone receptors is inhibited by the hsp90-specific compound geldanamycin. *J. Biol. Chem.* **272,** 18694–18701
32. Meacham, G. C., Patterson, C., Zhang, W., Younger, J. M., and Cyr, D. M. (2001) The Hsc70 co-chaperone CHIP targets immature CFTR for proteasomal degradation. *Nat. Cell Biol.* **3,** 100–105
33. Jha, K. N., Wong, L., Zerfas, P. M., De Silva, R. S., Fan, Y. X., Spiridonov, N. A., and Johnson, G. R. (2010) Identification of a novel HSP70-binding cochaperone critical to HSP90-mediated activation of small serine/threonine kinase. *J. Biol. Chem.* **285,** 35180–35187
34. Grad, I., Cederroth, C. R., Walicki, J., Grey, C., Barluenga, S., Winssinger, N., De Massy, B., Nef, S., and Picard, D. (2010) The molecular chaperone Hsp90α is required for meiotic progression of spermatocytes beyond pachytene in the mouse. *PLoS ONE* **5,** e15770
35. Lim, K. L., Chew, K. C., Tan, J. M., Wang, C., Chung, K. K., Zhang, Y., Tanaka, Y., Smith, W., Engelender, S., Ross, C. A., Dawson, V. L., and Dawson, T. M. (2005) Parkin mediates nonclassical, proteasomal-independent ubiquitination of synphilin-1. Implications for Lewy body formation. *J. Neurosci.* **25,** 2002–2009
36. Luthman, H., and Magnusson, G. (1983) High efficiency polyoma DNA transfection of chloroquine treated cells. *Nucleic acids research* **11,** 1295–1308
37. van de Kooij, B., Verbrugge, I., de Vries, E., Gijsen, M., Montserrat, V., Maas, C., Neefjes, J., and Borst, J. (2013) Ubiquitination by the membrane-associated RING-CH-8 (MARCH-8) ligase controls steady-state cell surface expression of tumor necrosis factor-related apoptosis inducing ligand (TRAIL) receptor 1. *J. Biol. Chem.* **288,** 6617–6628
38. Belle, A., Tanay, A., Bitincka, L., Shamir, R., and O'Shea, E. K. (2006) Quantification of protein half-lives in the budding yeast proteome. *Proc. Natl. Acad. Sci. U.S.A.* **103,** 13004–13009
39. La Salle, S., Sun, F., and Handel, M. A. (2009) Isolation and short-term culture of mouse spermatocytes for analysis of meiosis. *Methods Mol. Biol.* **558,** 279–297
40. Bellvé, A. R. (1993) Purification, culture, and fractionation of spermatogenic cells. *Methods Enzymol.* **225,** 84–113
41. Pedersen, A. G., and Nielsen, H. (1997) Neural network prediction of translation initiation sites in eukaryotes. Perspectives for EST and genome analysis. *Proc. Int. Conf. Intell. Syst. Mol. Biol.* **5,** 226–233

42. Ciechanover, A. (1998) The ubiquitin-proteasome pathway. on protein death and cell life. *EMBO J.* **17,** 7151–7160
43. Meng, L., Mohan, R., Kwok, B. H., Elofsson, M., Sin, N., and Crews, C. M. (1999) Epoxomicin, a potent and selective proteasome inhibitor, exhibits *in vivo* antiinflammatory activity. *Proc. Natl. Acad. Sci. U.S.A.* **96,** 10403–10408
44. Taipale, M., Krykbaeva, I., Koeva, M., Kayatekin, C., Westover, K. D., Karras, G. I., and Lindquist, S. (2012) Quantitative analysis of HSP90-client interactions reveals principles of substrate recognition. *Cell* **150,** 987–1001
45. Bucko-Justyna, M., Lipinski, L., Burgering, B. M., and Trzeciak, L. (2005) Characterization of testis-specific serine-threonine kinase 3 and its activation by phosphoinositide-dependent kinase-1-dependent signalling. *FEBS J.* **272,** 6310–6323
46. Baker, M. A., Smith, N. D., Hetherington, L., Pelzing, M., Condina, M. R., and Aitken, R. J. (2011) Use of titanium dioxide to find phosphopeptide and total protein changes during epididymal sperm maturation. *J. Proteome Res.* **10,** 1004–1017